Unusual nucleotide-binding properties of the chloroplast protein import receptor, atToc33

Henrik Aronsson[1], Jonathan Combe[1], Paul Jarvis*

Department of Biology, University of Leicester, University Road, Leicester LE1 7RH, UK

Received 4 April 2003; revised 22 April 2003; accepted 22 April 2003

First published online 12 May 2003

Edited by Ulf-Ingo Flügge

Abstract ***Arabidopsis*** **Toc33 (atToc33) is a GTP-binding protein of the chloroplast outer envelope membrane. We studied its nucleotide-binding properties in vitro, and found that it binds GTP, GDP and XTP, with similar efficiencies, but not ATP. We further demonstrated that atToc33 has intrinsic GTPase activity. Mutations within the putative G4 motif of the atToc33 nucleotide-binding domain (D217N, D219N and E220Q) had no effect on nucleotide specificity or GTPase activity. Similarly, a mutation in the newly assigned G5 motif (E208Q) did not affect nucleotide specificity or GTPase activity. Furthermore, the D217N and D219N mutations did not affect atToc33 functionality in vivo. The data demonstrate that atToc33 belongs to a novel class of GTPases with unusual nucleotide-binding properties.**

Key words: *Arabidopsis*; Chloroplast protein import; GTPase; *ppi1*; atToc33; XTP

1. Introduction

The majority of proteins within chloroplasts are nucleus encoded [1]. The mechanism for translocating nucleus-encoded proteins from the cytosol into the interior of chloroplasts involves translocons in the outer and inner envelope membranes called Toc and Tic, respectively [2,3]. Precursor proteins (preproteins) targeted to chloroplasts carry an N-terminal transit peptide that is recognised by the Toc complex prior to envelope translocation. The recognition of preproteins by the import apparatus has not been precisely defined, but it involves GTP-binding receptors in the outer envelope membrane called Toc34 and Toc159 [4–7]. Accordingly, GTP has been shown to have a positive effect on the early stages of chloroplast protein import in vitro [4,8]. Following recognition, preproteins are transferred to Toc75, a major constituent of the outer envelope translocation channel, and then translocated simultaneously across both envelope membranes. The transit peptide is cleaved upon arrival in the stroma, and the mature protein is then folded into its final conformation or targeted to one of several internal compartments [2,3].

There are currently two models for preprotein recognition by the Toc receptors. In the first, Toc159 and Toc34 remain stably associated with the outer envelope membrane and interact with incident preproteins directly, much like the mitochondrial protein import receptors, Tom20 and Tom22 [9]. In support of this model, preproteins can be cross-linked to Toc159 and Toc34 very early during import into isolated chloroplasts [10], and a direct and specific interaction between preproteins and Toc34 has been observed in vitro [11]. In the second model, soluble Toc159 binds to preproteins in the cytosol, and then mediates their targeting to the chloroplast surface by docking at membrane-bound Toc34 [12]. In support of this model, an abundant cytosolic form of Toc159 has been observed [12], and the crystal structure of Toc34 suggests that heterodimerisation between Toc34 and Toc159 may be possible [13]. This model is reminiscent of signal recognition particle (SRP)-dependent protein targeting, in which the GTP-binding protein, SRP54, initiates preprotein translocation by docking at receptors that are themselves GTP-binding proteins [14].

Attempts have been made to elucidate the roles of the Toc receptors by manipulating their activities using guanine nucleotide analogues [4,8]. However, it was not possible to attribute the effects of these manipulations to a single translocon component, since there are at least two different GTP-binding Toc proteins. In fact, at least five different GTP-binding Toc components have been identified in *Arabidopsis* [15,16]: two Toc34 homologues, atToc33 and atToc34, and at least three Toc159 homologues, atToc159, atToc132 and atToc120. To manipulate one of these Toc proteins independently of the others, one would first need to change its nucleotide specificity. Since steady-state concentrations of XTP and XDP are relatively low in cells [17], a change of specificity from guanine nucleotides to xanthine nucleotides would be particularly desirable.

GTP-binding proteins are characterised by the presence of several conserved sequence motifs (G1 to G4) within their nucleotide-binding domains [18]. The protein import receptors, Toc159 and Toc34, also appear to have these conserved sequence motifs [4,7], and mutations within the putative G1 (GGVGKS→RGVGNR) and G4 (NKND→NKKL) motifs of pea Toc34 (psToc34) have been shown to impair GTP binding [19]. Several studies using a variety of different GTP-binding proteins have demonstrated that nucleotide specificity can be changed from guanine nucleotides to xanthine nucleotides by a single Asp-to-Asn mutation within the G4 motif (NKXD→NKXN) [20–23]. To better understand the function of *Arabidopsis* atToc33 (the presumed orthologue of psToc34 [15]), we characterised its nucleotide-binding and -hydrolysing properties in vitro, and attempted to change its

*Corresponding author. Fax: (44)-116-252 3330.
E-mail address: rpj3@le.ac.uk (P. Jarvis).

[1] These authors contributed equally to this study.

0014-5793/03/$22.00
doi:10.1016/S0014-5793(03)00478-2

nucleotide specificity by mutating the putative G4 motif [4,7,19] and a recently assigned G5 motif [13].

2. Materials and methods

2.1. Bacterial overexpression and site-directed mutagenesis

Plasmid pRSET::atToc33 was created by ligating a polymerase chain reaction (PCR) product corresponding to amino acid residues 1–262 of *Arabidopsis thaliana* Toc33 (atToc33) [15] into pRSET B (Invitrogen). The PCR product was amplified from atToc33 cDNA [15] using forward (5′-GGAGCCATGGGGTCTCTCGTTCGTGAATG-3′) and reverse primers (5′-CTTTATCATCAGAGTAAGCTTCATCTACCATC-3′) that introduced *Nco*I and *Hin*dIII restriction sites at the 5′ and 3′ ends, respectively. The *Nco*I site was at the start codon, creating an in-frame fusion with six His codons located upstream of the pRSET B polylinker. The pRSET::atToc33 clone was confirmed by sequencing and introduced into *Escherichia coli* strain BL21-DE3 (Novagen). Soluble atToc33 protein lacking the transmembrane domain (atToc33ΔTM) was overexpressed by inducing mid-exponential phase cultures with 1 mM IPTG (isopropyl β-D-thiogalactoside), and purified under native conditions using Ni-NTA resin (Qiagen). atToc33ΔTM was eluted using 250 mM imidazole and dialysed against 10% (v/v) glycerol, 1 mM dithiothreitol, 50 mM Tris–HCl, pH 8.0, at 4°C overnight. The protein was quantified using Bradford reagent (Bio-Rad).

Point mutations were generated by overlap extension PCR [24] using pRSET::atToc33 as template. Primary amplification reactions were carried out using the following primer pairs: A1 (5′-TAGAGTCGATGAGCTAGATAAGC-3′) with A2 (5′-GTTCTTGCTGCATCTTCCGCTGTTC-3′); and B1 (the mutagenic primer) with B2 (5′-CTTTATCATCAGAGTAAGCTTCATCTACCATC-3′). The B1 primers used were: for atToc33^{D217N}, 5′-GGAAGATGCAGCAAGAACAACAAGGACGAAAAGG-3′; for atToc33^{D219N}, 5′-GGAAGATGCAGCAAGAACGATAAGAACGAAAAGG-3′; for atToc33$^{D217N/D219N}$, 5′-GGAAGATGCAGCAAGAACAACAAGAACGAAAAGG-3′; for atToc33$^{D219N/E220Q}$, 5′-GGAAGATGCAGCAAGAACGATAAGAACCAGAAGG-3′; and for atToc33^{E208Q}, 5′-GCACAGAACAGCGGAAGATGC-3′. Following gel isolation, the primary amplification products were used as template for the overlap extension PCR reactions using primers A1 and B2. The overlap extension amplification products were cloned into pRSET::atToc33 as *Bst*XI–*Hin*dIII fragments, replacing the wild-type sequence, and the presence of each mutation was confirmed by sequencing.

Plasmid pET14b encoding wild-type, hexahistidinyl-tagged Rab5 [21] was introduced into *E. coli* strain BL21-DE3 for the expression of Rab5 protein. Expression and purification of Rab5 was carried out as described for atToc33ΔTM.

2.2. Nucleotide-binding assays

Nucleotide analogues carrying the *N*-methyl-3′-*O*-anthraniloyl (*mant*) fluorophore were used [25]. Binding buffer contained 10% (v/v) glycerol, 5 mM $MgCl_2$, 2 mM dithiothreitol and 50 mM Tris–HCl, pH 8.0. Fluorescence measurements were recorded using a fluorescence spectrophotometer (Varian Eclipse). Excitation was at 350 nm (10 nm slit), and emission was recorded between 400 nm and 600 nm. Fluorescence spectra were recorded 0 min (T_0) and 7 min (T_7) after adding 3 μM protein to 0.1 μM *mant*-ATP, 0.1 μM *mant*-GTP, 0.1 μM *mant*-GDP or 0.1 μM *mant*-XTP (Jena Bioscience). Spectra were adjusted so that fluorescence values at 600 nm were equal to zero, and then normalised so that T_0 fluorescence maxima were equal to one. Difference spectra (400–540 nm) were obtained by subtracting the T_0 values from the T_7 values.

2.3. GTP-hydrolysis assays

atToc33ΔTM protein (0.1 μg) was incubated with 1 μCi [α-^{32}P]GTP (3000 Ci/mmol; NEN) at 37°C in 10 μl buffer (50 mM NaCl, 2 mM dithiothreitol, 1 mM $MgCl_2$, 20 mM Tricine–KOH, pH 7.6); for competition experiments, unlabelled nucleotides were added prior to the addition of atToc33ΔTM protein at the indicated concentrations. Aliquots (1 μl) were removed after 5, 15, 30 and 60 min, spotted onto PEI-cellulose thin layer chromatography (TLC) strips (Macherery-Nagel), and separated using 600 mM $Na_2H_2PO_4$, pH 3.4. Dried strips were exposed to X-ray film, and the bands were quantified using ImageQuant software (Molecular Dynamics).

2.4. Genetic complementation studies

A 6.5 kb *Xba*I fragment carrying the complete atToc33 gene [15] was ligated into pUC19 to create pUC::atToc33g. Codon changes were generated by overlap extension PCR mutagenesis, using pUC::atToc33g as template. The primary amplification reactions were carried out using the following primer pairs: A1 with A2; and B1 (for atToc33^{D217N} and atToc33^{D219N}) with C2 (5′-CCTCTTCTTCAGAGCCTCTTAAA-3′). The overlap extension amplification reactions were carried out with primers A1 and C2. The products were cloned in pGEM-T Easy (Promega) and verified by sequencing. Mutant *Bst*XI–*Eco*RV fragments from the pGEM-T clones were used to replace the corresponding wild-type sequence in pUC::atToc33g, creating pUC::atToc33g^{D217N} and pUC::atToc33g^{D219N}, and the mutations were confirmed by sequencing. Finally, 6.5 kb *Xba*I genomic fragments from pUC::atToc33g^{D217N} and pUC::atToc33g^{D219N} were introduced into plant transformation vector, pPZP221 [26], to create pPZP::atToc33g^{D217N} and pPZP::atToc33g^{D219N}. These two constructs were used to transform *plastid protein import 1* (*ppi1*) mutant *Arabidopsis* plants by floral dipping [15,27].

Transgenic plants were selected by plating the T_1 generation on Murashige and Skoog medium (Sigma) containing 0.5% (w/v) sucrose, 110 μg/ml (w/v) gentamicin sulphate and 200 μg/ml (w/v) cefotaxime sodium; in vitro plant growth procedures were as described previously [28]. Gentamicin-resistant seedlings were transferred to soil after 14 day and allowed to set seed. To confirm the presence of the atToc33 transgenes, DNA isolated from T_2 seedlings [29] was analysed by PCR using the transgene-specific primers, C1 (5′-GGTCTCTCGTTCGTGAATGG-3′) and C2. The presence of the mutations was confirmed by sequencing the PCR products. Homozygosity at the *ppi1* T-DNA insertion was confirmed by plating T_2 seed on medium containing 50 μg/ml (w/v) kanamycin monosulphate [15].

Genetic complementation of the *ppi1* mutation was quantified by measuring the chlorophyll content of T_2 plants. Cotyledons from 14- to 16-day-old wild-type, *ppi1*, *ppi1*/atToc33g^{D217N} and *ppi1*/atToc33g^{D219N} plants grown in vitro were incubated in DMF (*N*,*N*′-dimethylformamide) in the dark at 4°C overnight. Chlorophyll was determined by measuring absorbance at 646.8 and 663.8 nm and calculated as described previously [30]. Expression of atToc33 in these T_2 lines was confirmed by immunoblotting using standard procedures and an atToc33-specific polyclonal antibody raised against the C-terminal peptide, CQGAIRNDIKTSGKPL (Eurogentec); an antibody raised against pea Tic110 was used as a loading control. The secondary antibody was an anti-rabbit IgG alkaline phosphatase conjugate (Sigma), and the detection reagent was BCIP/NBT alkaline phosphatase substrate (Sigma).

3. Results and discussion

3.1. Nucleotide-binding properties of wild-type atToc33ΔTM

Hexahistidinyl-tagged atToc33 lacking the C-terminal transmembrane domain (atToc33ΔTM) was overexpressed in *E. coli* and purified by affinity chromatography. The purified protein (expected size ~33 kDa) was analysed by sodium dodecyl sulfate–polyacrylamide gel electrophoresis (SDS–PAGE) and estimated to be >90% pure (Fig. 1B, lane 2). To investigate the nucleotide-binding properties of the atToc33ΔTM protein, we used an *N*-methyl-3′-*O*-anthraniloyl (*mant*)-nucleotide-binding assay. The *mant* moiety is a fluorophore that responds with different intensities and wavelengths of fluorescence depending on the hydrophobicity of its surroundings [25]. Free and bound forms of *mant*-nucleotides can therefore be distinguished using a fluorescence spectrophotometer, enabling the study of protein–nucleotide interactions in vitro. Excitation at 350 nm gives rise to a fluorescence emission peak at ~450 nm with unbound *mant*-nucleotides, and a more intense peak at ~430 nm with bound nucleotides. When atToc33ΔTM protein was added to *mant*-GTP or *mant*-GDP, a robust increase in fluorescence and a blue-shift in the emission maximum was observed after 7 min, indicating that a strong protein–nucleotide interaction had occurred in each

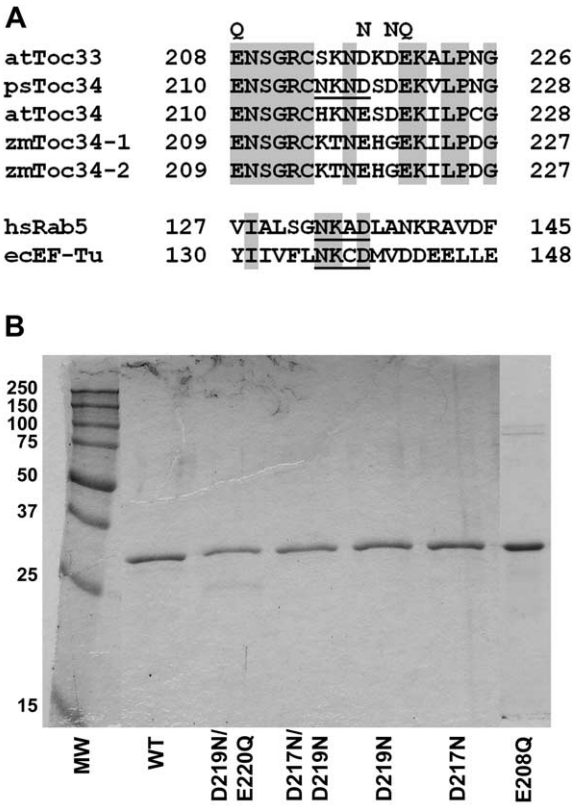

Fig. 1. Sequence alignment and SDS–PAGE analysis of recombinant proteins. A: The putative G4 regions of Toc34-related proteins from *Arabidopsis* (at), pea (ps) and maize (zm) are shown aligned. Residues conserved in all sequences are shaded, and the proposed G4 motif of psToc34 is underlined. The different mutations introduced into atToc33 (D217N, D219N, E220Q and E208Q) are shown above the alignment. For comparison, the G4 regions of human (hs) Rab5 and *E. coli* (ec) EF-Tu are also shown. B: Recombinant atToc33ΔTM proteins (WT, D219N/E220Q, D217N/D219N, D219N, D217N and E208Q) were resolved by SDS–PAGE and stained with Coomassie. Each lane holds ~1 μg protein. Molecular weight standards (MW) are indicated in kDa.

case; these data are expressed as difference spectra in Fig. 2A. To assess the specificity of this interaction, we tested the ability of atToc33ΔTM to bind *mant*-ATP. As expected, no evidence for an atToc33–ATP interaction was observed (Fig. 2A). However, when we conducted a similar assay using *mant*-XTP, a strong atToc33–XTP interaction was clearly seen (Fig. 2A).

It is clear from the data that wild-type atToc33 protein binds GTP, GDP and XTP with similar efficiencies, and that the observed atToc33–GTP/GDP/XTP interactions are specific since no evidence for an atToc33–ATP interaction was observed. The finding that atToc33 binds XTP as efficiently as it binds GTP/GDP is surprising, since most other GTP-binding proteins tested have been found to bind GTP several orders of magnitude more efficiently than XTP [20–23]. To confirm that this result was not an artefact of our experimental procedure, we analysed a canonical GTP-binding protein, human Rab5, using exactly the same protocol. Increased fluorescence was observed in the Rab5–GTP assay, but not in the Rab5–XTP assay (data not shown). Since Rab5 was previously shown to bind GTP but not XTP, these results confirm the validity of the experimental procedure employed here.

The strong sequence similarity between atToc33 and psToc34 (~60% amino acid sequence identity) suggests that the proteins may behave similarly with respect to nucleotide binding. Indeed, several previous studies have shown that psToc34 does not bind ATP [4,7,11]. The inability of atToc33 (or psToc34) to bind ATP is significant with regard to its role in chloroplast protein import. The translocation of preproteins across the outer envelope membrane requires low concentrations of ATP (< 100 μM) [8,28], but the site of ATP consumption remains to be determined. Since atToc33 (or psToc34) does not bind ATP in vitro, it is unlikely that it is responsible for this ATP requirement.

3.2. *Nucleotide-binding properties of atToc33ΔTM G4 mutants*

In an attempt to change atToc33 nucleotide specificity (and make the protein more discriminatory in favour of xanthine nucleotides), selected residues within the putative G4 motif of its nucleotide-binding domain were mutated. In canonical GTP-binding proteins, the carboxyl side chain of the G4 Asp makes hydrogen bonds with NH1 and the exocyclic 2-amino group of the guanine base. Previous studies using several different GTP-binding proteins demonstrated that mutation of the G4 Asp to Asn results in a change of specificity from guanine nucleotides to xanthine nucleotides [20–23]. In these G4 mutants, the amide side chain of the new Asn residue is predicted to make hydrogen bonds with NH1 and the 2-carbonyl group of the xanthine base. Because the putative G4 motif originally identified in psToc34 (residues 216–219) [4,7,19] is not well conserved in other Toc34-related proteins (Fig. 1A), three different residues that may play a role in determining atToc33 nucleotide specificity were mutated: (1) Asp 217, since it corresponds exactly to Asp 219 of the putative psToc34 G4 motif; (2) Asp 219, since the sequence NDKD matches the G4 consensus (NKXD) more closely; and (3) Glu 220, since it is conserved in all five Toc34-related sequences. An analysis of ~70 different GTP-binding proteins demonstrated that significant deviations from the NKXD consensus are possible [18]; for example, the G4 motifs of *Saccharomyces cerevisiae* RHO2 and CDC42 are LKKD and TQID, respectively.

Four putative atToc33 G4 mutants (D217N, D219N, D217N/D219N and D219N/E220Q; Fig. 1A) were generated by overlap extension PCR and cloned into the pRSET expression vector. Hexahistidinyl-tagged mutant atToc33ΔTM proteins were overexpressed in *E. coli* and purified by affinity chromatography. All of the proteins were estimated to be > 90% pure by SDS–PAGE (Fig. 1B, lanes 3–6). The nucleotide-binding properties of each mutant protein were determined as described for the wild-type protein, and the data are presented as difference spectra (Fig. 2B–E). It is clear from the data that all of the mutants have essentially the same nucleotide-binding properties as wild-type atToc33, and that none of the selected residues is important for determining atToc33 nucleotide specificity.

Evidence was recently presented that a psToc34 D219N mutation (the equivalent of the atToc33 D217N mutation) does have a slight effect on nucleotide specificity [31]. As described above, these results are not supported by our data (Fig. 2A,B). However, our results are fully consistent with conclusions drawn from the crystal structure of psToc34 [13], which indicated that the Asp 219 side chain is totally exposed to the solvent [13]. Instead, the carboxyl side chain

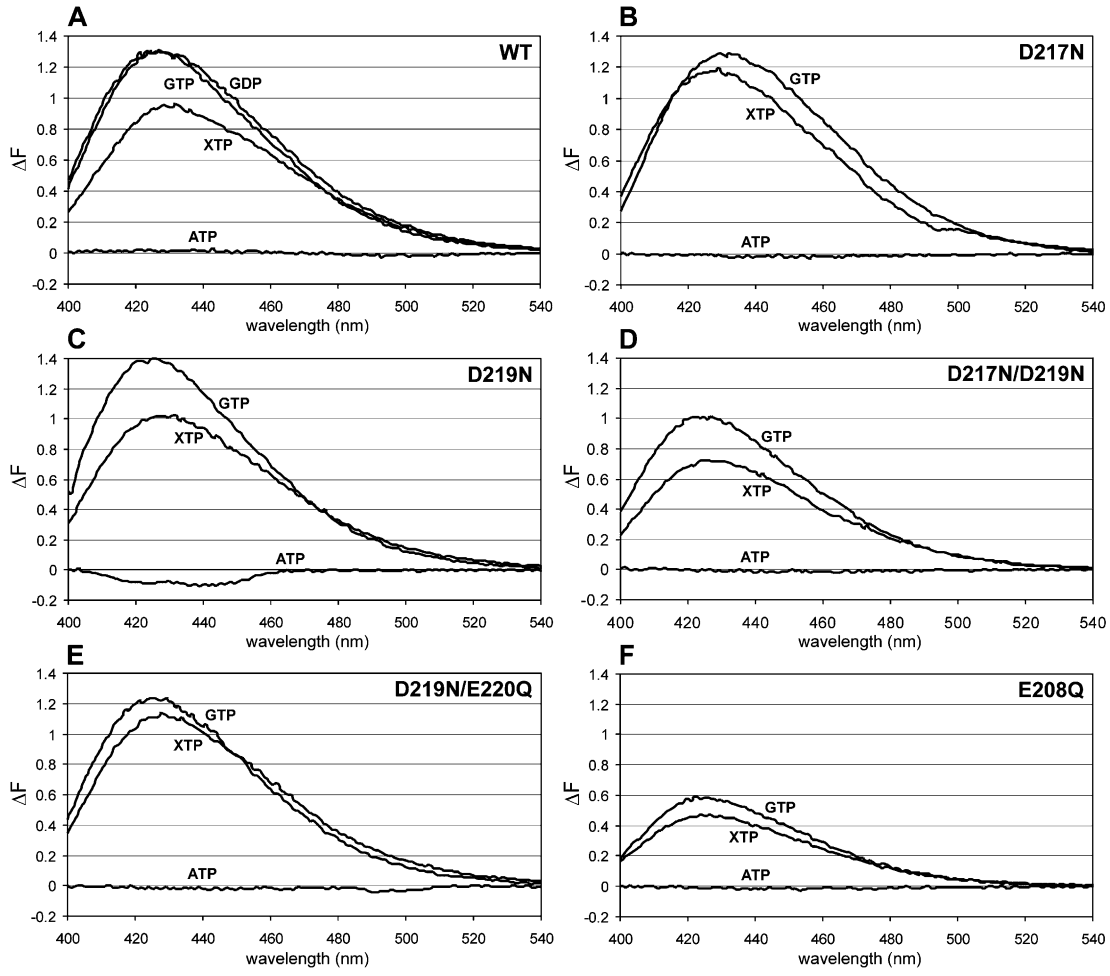

Fig. 2. Nucleotide-binding assays. Binding assays using wild-type (A) and mutant (B–F) recombinant atToc33ΔTM proteins, and either *mant*-GTP, *mant*-GDP (wild type only), *mant*-XTP or *mant*-ATP, were conducted. Fluorescence spectra were recorded 0 min (T_0) and 7 min (T_7) after the initiation of each binding assay, normalised, and then used to derive fluorescence difference (ΔF) spectra by subtracting the T_0 values from the T_7 values. The presented data are representative of at least three independent experiments.

of Glu 210 was predicted to make one strong and one weak hydrogen bond with NH1 and the 2-amino group of guanine, respectively, and this residue was therefore assigned to a new G5 motif [13]. We assessed the role of the corresponding atToc33 residue (Glu 208; Fig. 1A) in determining nucleotide specificity, but found that purified atToc33ΔTM^{E208Q} (Fig. 1B, lane 7) bound GTP and XTP with similar efficiencies (Fig. 2F), just like the wild-type protein (Fig. 2A). Because wild-type atToc33ΔTM is able to bind both GTP and XTP, and because atToc33ΔTM^{E208Q} does not show any preference for XTP over GTP, we conclude that only the NH1 hydrogen bond plays a significant role in nucleotide binding. Interestingly, the ΔF values obtained for atToc33ΔTM^{E208Q} (GTP: 0.59 ± 0.05, XTP: 0.54 ± 0.11; $n = 5$) were significantly lower than those obtained for the wild type (GTP: 1.19 ± 0.10, XTP: 1.09 ± 0.09; $n = 3$). This most likely indicates weaker nucleotide binding by atToc33ΔTM^{E208Q} caused by a reduction in the strength of the NH1 hydrogen bond, and is consistent with a role for Glu 208 in nucleotide binding.

3.3. *Wild-type atToc33ΔTM and the G4 mutants have intrinsic GTPase activity*

The ability of atToc33 to hydrolyse GTP has not been studied in any detail, and there is some disagreement in the literature concerning the ability of psToc34 to hydrolyse GTP [7,11,13]. We therefore conducted a GTP-hydrolysis assay using wild-type atToc33ΔTM protein. The result, shown in Fig. 3A (left panel), clearly demonstrates that atToc33 has intrinsic GTPase activity. To confirm that the GTPase activity was attributable to atToc33 and not some contaminating *E. coli* protein, we conducted an identical GTP-hydrolysis assay using a control protein that does not bind GTP (atTic22-IV) and which was purified using a similar procedure; as expected, no GTP hydrolysis was observed (data not shown). The fact that purified atToc33 protein is able to hydrolyse GTP demonstrates that a separate GTPase-activating protein (GAP) is not absolutely required, and is consistent with the hypothesis that Toc34-related proteins form dimers in which each partner acts as the other partner's GAP [13].

There are some reports in the literature of G4 Asp-to-Asn mutations that do not result in a change of nucleotide specificity [32,33]. In the case of methylation-dependent restriction endonuclease subunit, McrB, the G4 Asp-to-Asn mutation resulted in dramatically reduced GTPase activity [33]. To determine if the atToc33 G4 and G5 mutations affect GTPase activity, we conducted GTP-hydrolysis assays using each mu-

tant atToc33ΔTM protein. All five atToc33 mutants were found to have similar GTPase activities to that of the wild-type protein, but only the data obtained using atToc33-ΔTM^{D217N}, atToc33ΔTM$^{D219N/E220Q}$ and atToc33ΔTM^{E208Q} are shown (Fig. 3A). Quantification of the data revealed no significant differences in reaction kinetics between the different GTP-hydrolysis assays (Fig. 3B). The observation that the D217N mutation does not affect GTPase activity is inconsistent with a previous study on an equivalent psToc34 mutant (D219N) [31], but is fully consistent with the nucleotide-binding data presented earlier (Fig. 2) and with the crystal structure of psToc34 [13]. Because the effect of E208Q on nucleotide binding (Fig. 2) does not significantly influence GTPase activity, we can conclude that the hydrolysis reaction rather than nucleotide binding is rate limiting for atToc33 GTPase activity.

To corroborate our findings on atToc33 nucleotide binding and specificity, we conducted GTP-hydrolysis assays in the presence of different concentrations of cold competitor nucleotides (Fig. 3C,D). We found that GTP and XTP were equally effective as competitors in assays using wild-type atToc33ΔTM. This is consistent with our earlier observation that wild-type atToc33ΔTM binds *mant*-GTP and *mant*-XTP with similar efficiencies (Fig. 2A). Furthermore, we observed that XTP was no more effective as a competitor in GTP-hydrolysis assays using the different G4 and G5 mutants than in those using wild-type atToc33ΔTM (Fig. 3C,D). This confirms our previous conclusion that none of the mutations has a significant effect on nucleotide specificity in vitro. In each competition experiment, the degree of inhibition of GTPase activity observed was similar to that reported previously for psToc34 [31].

3.4. Full-length atToc33 G4 mutants are functional in vivo

Because all of the assays on the atToc33 mutants described so far were conducted in vitro using C-terminally truncated proteins, we tested the activity of two full-length mutant proteins in vivo. To do this we used a transgenic complementation assay based on the *Arabidopsis* atToc33 knockout mutant, *ppi1* [15]. The D217N and D219N mutations were introduced into a genomic clone of the atToc33 gene without altering any of the introns or the 5′ and 3′ regulatory regions. These constructs were used to transform *ppi1* plants, and genetic complementation of the *ppi1* mutation was assessed in the T_2 generation. The *ppi1* mutant is chlorophyll deficient as a result of its chloroplast protein import defect, and so com-

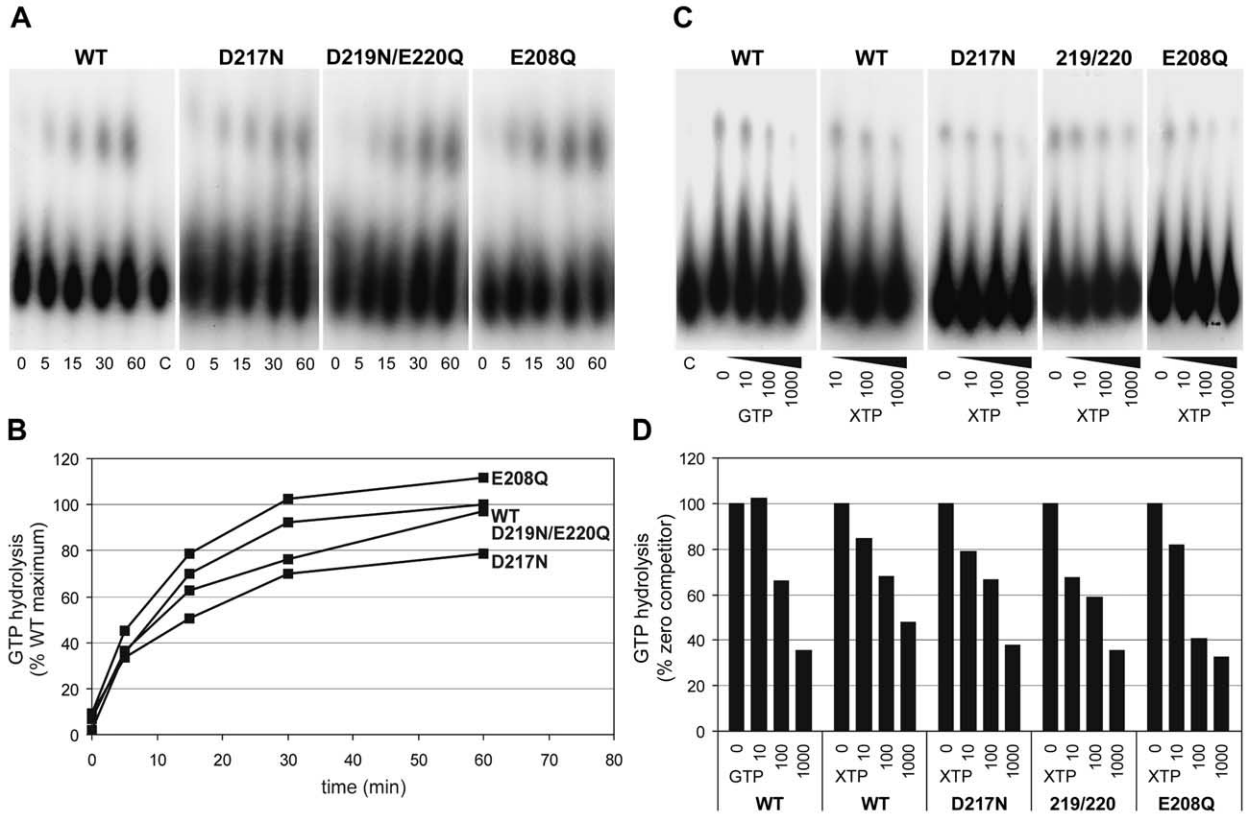

Fig. 3. GTP-hydrolysis assays. A: Wild-type (WT) and mutant (D217N, D219N/E220Q and E208Q) recombinant atToc33ΔTM proteins were incubated with [α-^{32}P]GTP for 5, 15, 30 and 60 min. The samples were then separated by TLC and visualised by autoradiography. The lower band in each case corresponds to unhydrolysed GTP, and the upper band corresponds to GDP. No hydrolysis was observed in a control reaction (C) lacking recombinant protein. B: Radioactivity associated with each band in panel A was quantified and used to calculate the degree of GTP hydrolysis at each time-point; each value is expressed as a percentage of the wild-type atToc33ΔTM 60 min value. C: Similar GTP-hydrolysis assays were conducted in the presence of different concentrations of cold competitor (GTP or XTP, as indicated). Ten-, 100- and 1000-fold excesses of competitor were employed as shown. Each assay was incubated for 15 min. Once again, no hydrolysis was observed in a control reaction (C) lacking recombinant protein. D: Radioactivity associated with each GDP band in panel C was quantified and used to calculate the degree of GTP hydrolysis in each experiment; each value is expressed as a percentage of the value obtained in the absence of competitor using the corresponding protein. All of the presented data are representative of at least two independent experiments.

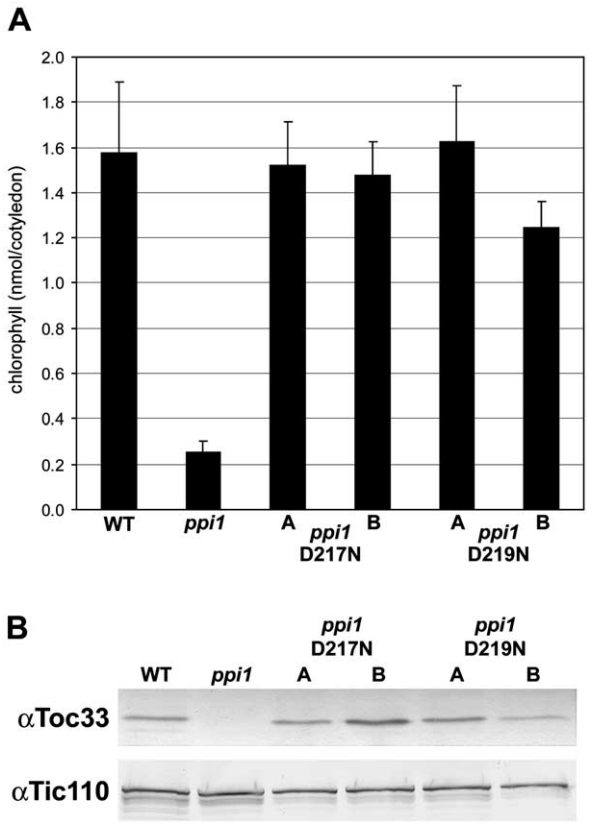

Fig. 4. Genetic complementation assays. A: The abilities of two putative atToc33 G4 mutants (D217N and D219N) to complement the chlorophyll deficiency of the atToc33 knockout mutant, *ppi1*, were assessed in transgenic assays. Chlorophyll data from wild-type plants, untransformed *ppi1* plants, and transgenic *ppi1* plants (T_2 generation) carrying each of the atToc33 mutants are presented. Data from two independent transformants (A and B) are shown for each G4 mutation. B: Expression of the atToc33 transgenes in these T_2 lines was confirmed by immunoblotting using an atToc33-specific antibody. Sample loadings were controlled using an antibody raised against Tic110, a component of the Tic complex.

plementation of the mutation can easily be assessed by measuring the chlorophyll content of plants [15]. As shown in Fig. 4A, both atToc33^{D217N} and atToc33^{D219N} efficiently complemented the *ppi1* chlorophyll deficiency, demonstrating that the putative G4 mutations have no significant effect on the in vivo functionality of full-length atToc33 protein. Complementation of the chlorophyll phenotype correlated with restored expression of the atToc33 protein at levels comparable to those present in the wild type (Fig. 4B). Because these in vivo data are fully consistent with the in vitro data for atToc33ΔTM^{D217N} and atToc33ΔTM^{D219N} described earlier (Figs. 2 and 3), it seems unlikely that any of the other mutants would behave differently in vivo.

4. Conclusions

We have analysed the nucleotide-binding and -hydrolysing properties of atToc33 in detail for the first time. We found that atToc33, like psToc34, binds GTP and GDP but not ATP. Purified atToc33 was also shown to have intrinsic GTPase activity, demonstrating that a separate GAP is not absolutely required. Surprisingly, atToc33 was found to bind XTP with approximately the same efficiency as GTP and GDP. Furthermore, mutations within the putative specificity-determining G4 and G5 motifs of atToc33 did not affect nucleotide specificity, GTPase activity, or (in the case of D217N and D219N) in vivo functionality. Taken together, these data demonstrate that atToc33 belongs to a novel class of GTPases with unusual nucleotide-binding properties, and support the conclusions drawn from the crystal structure of psToc34 [13].

Acknowledgements: We thank Anthony Wardle and Ramesh Patel for technical assistance, Penny Dudley for constructing pRSET::atToc33, Nigel Scrutton for the use of the fluorescence spectrophotometer, Kirill Alexandrov for the pET14b Rab5 cDNA clone, and Kenneth Keegstra for the Tic110 antibody. This work was supported by a Wenner-Gren Foundation Fellowship (to H.A.), the Royal Society Rosenheim Research Fellowship (to P.J.), and Biotechnology and Biological Sciences Research Council grants 91/C12976 and 91/P12928 (to P.J.).

References

[1] Abdallah, F., Salamini, F. and Leister, D. (2000) Trends Plant Sci. 5, 141–142.
[2] Jarvis, P. and Soll, J. (2001) Biochim. Biophys. Acta 1541, 64–79.
[3] Keegstra, K. and Cline, K. (1999) Plant Cell 11, 557–570.
[4] Kessler, F., Blobel, G., Patel, H.A. and Schnell, D. (1994) Science 266, 1035–1039.
[5] Schnell, D., Kessler, F. and Blobel, G. (1994) Science 266, 1007–1012.
[6] Hirsch, S., Muckel, E., Heemeyer, F., von Heijne, G. and Soll, J. (1994) Science 266, 1989–1992.
[7] Seedorf, M., Waegemann, K. and Soll, J. (1995) Plant J. 7, 401–411.
[8] Young, M.E., Keegstra, K. and Froehlich, J.E. (1999) Plant Phys. 121, 237–243.
[9] Pfanner, N. and Geissler, A. (2001) Nat. Rev. Mol. Cell Biol. 2, 339–349.
[10] Kouranov, A. and Schnell, D. (1997) J. Cell Biol. 139, 1677–1685.
[11] Sveshnikova, N., Soll, J. and Schleiff, E. (2000) Proc. Natl. Acad. Sci. USA 97, 4973–4978.
[12] Hiltbrunner, A., Bauer, J., Vidi, P.-A., Infanger, S., Weibel, P., Howvy, M. and Kessler, F. (2001) J. Cell Biol. 154, 309–316.
[13] Sun, Y.-J., Forouhar, F., Li, H.-m., Tu, S.-L., Yeh, Y.-H., Kao, S., Shr, H.-L., Chou, C.-C., Chen, C. and Hsiao, C.-D. (2002) Nat. Struct. Biol. 9, 95–100.
[14] Keenan, R.J., Freymann, D.M., Stroud, R.M. and Walter, P. (2001) Annu. Rev. Biochem. 70, 755–775.
[15] Jarvis, P., Chen, L.-J., Li, H.-m., Peto, C.A., Fankhauser, C. and Chory, J. (1998) Science 282, 100–103.
[16] Bauer, J., Chen, K.H., Hiltbunner, A., Wehrli, E., Eugster, M., Schnell, D. and Kessler, F. (2000) Nature 403, 203–207.
[17] Henderson, J.F. and Paterson, A.R.P. (1973) Nucleotide Metabolism, pp. 97–169, Academic press, New York.
[18] Bourne, H.R., Sanders, D.A. and McCormick, F. (1991) Nature 349, 117–127.
[19] Chen, D. and Schnell, D.J. (1997) J. Biol. Chem. 272, 6614–6620.
[20] Hwang, Y.W. and Miller, D.L. (1987) J. Biol. Chem. 262, 13081–13085.
[21] Rybin, V., Ullrich, O., Rubino, M., Alexandrov, K., Simon, I., Seabra, M.C., Goody, R. and Zerial, M. (1996) Nature 383, 266–269.
[22] Schmidt, G., Lenzen, C., Simon, I., Deuter, R., Cool, R.H., Goody, R.S. and Wittinghofer, A. (1996) Oncogene 12, 87–96.
[23] Powers, T. and Walter, P. (1995) Science 269, 1422–1424.
[24] Vallejo, A.N., Pogulis, R.J. and Pease, L.R. (1995) in: PCR Primer: A Laboratory Manual (Dieffenbach, C.W. and Dveksler, G.S., Eds.), pp. 603–612, Cold Spring Harbor Laboratory Press, Cold Spring Harbor, NY.
[25] John, J., Sohmen, R., Feuerstein, J., Linke, R., Wittinghofer, A. and Goody, R.S. (1990) Biochemistry 29, 6058–6065.
[26] Hajdukiewicz, P., Svab, Z. and Maliga, P. (1994) Plant Mol. Biol. 25, 989–994.

[27] Clough, S.J. and Bent, A.F. (1998) Plant J. 16, 735–743.
[28] Aronsson, H. and Jarvis, P. (2002) FEBS Lett. 529, 215–220.
[29] Edwards, K., Johnstone, C. and Thompson, C. (1991) Nucleic Acids Res. 19, 1349.
[30] Porra, R.J., Thompson, W.A. and Kriedemann, P.E. (1989) Biochem. Biophys. Acta 975, 384–394.
[31] Jelic, M., Sveshnikova, N., Motzkus, M., Hörth, P., Soll, J. and Schleiff, E. (2002) Biol. Chem. 383, 1875–1883.
[32] Yu, B., Slepak, V.Z. and Simon, M.I. (1997) J. Biol. Chem. 272, 18015–18019.
[33] Pieper, U., Schweitzer, T., Groll, D.H., Gast, F.U. and Pingoud, A. (1999) J. Mol. Biol. 292, 547–556.